Journal of the Oceanographical Society of Japan
Vol. 29, pp. 94 to 105, 1973

Irrotational, Progressive Surface Gravity Waves near the Limiting Height*

Ken SASAKI** and Takashi MURAKAMI**

Abstract: Numerical solutions of irrotational, progressive surface gravity waves in water of a constant depth are obtained by means of an iterative method. Our results suggest that waves with the surface slope angle greater than $\pi/6$ may exist. The calculated phase velocity of deep water waves near the wave steepness 0.14 is significantly smaller than the value given by the Stokes' fourth approximation.

In order to check our method, we apply it to the problem proposed by DAVIES (1951), which is hypothetical but similar to the present problem, and for which the exact solution is known. In this case our results show good agreement with the exact solution.

1. Introduction

The properties of the highest waves in water of a constant depth (including an infinite depth) have been studied by MICHELL (1893), MCCOWAN (1894), YAMADA (1957), CHAPPELEAR (1959), and LENAU (1966). They determined the height and the phase velocity assuming that the limiting waves have pointed crests. Their results show that the solitary wave has the maximum height about 0.83 to 0.85 times the depth and that the maximum wave steepness of deep water waves is about 0.141.

In recent years several numerical works on large amplitude waves have been published. In a pioneering work by CHAPPELEAR (1961) the expansion coefficients of the velocity and and those of the wave form are determined by the method of least squares. VON SCHWIND and REID (1972) improved this method. The numerical method used by BYATT-SMITH (1970) is simpler and more attractive than the method of least squares. But he met a serious difficulty when the Froude number is greater than 1,293. FENTON (1972) used a method which is partly analytical and partly numerical, and which is promising if an extension to an order higher than nine is practicable.

Compared with the three numerical methods cited above, our method is simple and can provide a very dense distribution of points in order to represent the solutions near the limiting condition. Furthermore, the reliability of our method can be tested by applying it to a problem whose exact solution is known.

The purpose of the present paper is to describe our method of iteration which is applied to the equation derived by YAMADA (1958), and to study the properties of the steepest waves for which this method is valid. Our attention is concentrated not on the wave form but on the surface slope angle, because the latter plays an important role in analytical theories of the steepest physically stable waves.

2. Formulation

We use a co-ordinate system in which a progressive wave is reduced to a steady flow. A steady, incompressible, irrotational velocity field is represented by

$$u-iv=\frac{d(\phi+i\psi)}{d(x+iy)}=Ue^{\tau-i\theta} \qquad (1)$$

or

$$\frac{u+iv}{u^2+v^2}=\frac{d(x+iy)}{d(\phi+i\psi)}=\frac{1}{U}e^{-\tau+i\theta} \qquad (2)$$

where all symbols denote real quantities, and complex variables are analytic functions of an independent variable ζ to be introduced later.

* Received December 16, 1972
** Geophysical Institute, Faculty of Science, University of Tokyo, Bunkyo-ku, Tokyo, 113 Japan

u, v, x, y, ϕ, ψ and θ denote a horizontal velocity, a vertical velocity, a horizontal co-ordinate, a vertical co-ordinate, a velocity potential, a stream function, and the slope angle of streamlines, respectively. τ is a quantity proportional to $\log(u^2+v^2)$, and U is a constant with the dimension of velocity. These symbols are the same as used in page 523 of 'Water Waves' (STOKER, 1957).

On the free surface ψ is a constant, and the Bernouilli's equation gives

$$\frac{1}{2}(u^2+v^2)+gy=\text{const.} \qquad (3)$$

where g is the acceleration of gravity. We differentiate (3) with respect to ϕ, and use (2) to obtain

$$\frac{\partial\tau}{\partial\phi}=-\frac{g}{U^3}e^{-3\tau}\sin\theta \qquad (4)$$

YAMADA (1958) introduced an independent variable ζ defined by

$$\left.\begin{aligned}&\frac{d(\phi+i\psi)}{d\zeta}=U\cdot L_0\cdot M(\zeta)\\&M(\zeta)=i/\sqrt{\zeta(\zeta-a)(1-a\zeta)}\\&(-1\leqq a\leqq 0)\end{aligned}\right\} \qquad (5)$$

where a is a real parameter related to the relative depth, and L_0 is a constant with the dimension of length. We have on the real axis ($\mathrm{Im}(\zeta)=+0$)

$$\left.\begin{aligned}&\mathrm{Arg}(M)=\pi/2 \quad \text{for} \quad 0<\zeta\\&\mathrm{Arg}(M)=0 \quad \text{for} \quad a<\zeta<0\\&\text{and}\\&\mathrm{Arg}(M)=-\pi/2 \quad \text{for} \quad -1<\zeta<a\end{aligned}\right\} \qquad (6)$$

On the unit circle we have

$$M(\zeta)d\zeta=-d\sigma/\sqrt{1+a^2-2a\cos\sigma} \qquad (7)$$

where σ is the argument of ζ. It is obvious from (6) and (7) that the upper half of the unit circle in the ζ plane is mapped by (5) into a rectangle in the $\phi+i\psi$ plane, as shown in

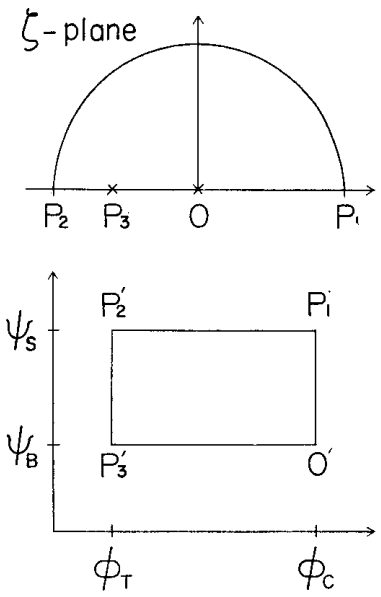

Fig. 1. Conformal mapping proposed by YAMADA. The upper half of a unit circle in the ζ plane passing through the points O, P_1, P_2 and P_3 is mapped into a rectangle in the $\phi+i\psi$ plane going through the corresponding points O', P'_1, P_2' and P_3'. Subscripts C, T, S and B denote crest, trough, surface, and bottom, respectively.

Figure 1, where subscripts C, T, S and B denote the crest, trough, surface, and bottom, respectively. Since $|\zeta|=1$ corresponds by assumption to a free surface in the $x+iy$ plane, (4), (5), (6) and (7) give

$$\frac{d\tau}{\alpha\sigma}=\left(\frac{gL_0}{U^2}\right)\frac{e^{-3\tau}\sin\theta}{\sqrt{1+a^2-2a\cos\sigma}} \qquad (8)$$

The ratio $(\psi_S-\psi_B)/2(\phi_C-\phi_T)$ is equal to the ratio of the water depth to the wave length of infinitesimal waves. The dependence of this ratio on a is found from numerical integrations of

$$\phi_C-\phi_T=U\cdot L_0\int_0^{\pi}\frac{d\sigma}{\sqrt{1+a^2-2a\cos\sigma}} \qquad (9)$$

and

$$i(\psi_S-\psi_B)=U\cdot L_0\int_0^1 M(\zeta)d\zeta \qquad (10)$$

In the case $a=0$ (deep water) we have $\phi_C-\phi_T=U\cdot L_0\cdot\pi$ and in the case $a=-1$ (solitary waves) we have $\phi_S-\phi_B=U\cdot L_0\cdot\pi/2$.

YAMADA assumed that

$$\tau(\bar{\zeta})-i\theta(\bar{\zeta})=\tau)\zeta)+i\theta(\zeta) \qquad (11)$$

Since the real axis in the ζ plane corresponds to one streamline and two equipotential lines in the $\phi+i\psi$ plane, this assumption leads both to the symmetry of the wave form and to the fact that the bottom is a flat horizontal plane.

Thus our problem is to find analytic functions $\tau-i\theta$ whose boundary condition on $|\zeta|=1$ is given by Equation (8). Furthermore, they are regular in $|\zeta|\leqq 1$ and satisfy (11).

3. Transformation from $d\tau/d\sigma$ to θ

An analytic function $\tau-i\theta$ is represented by an infinite power series

$$\tau-i\theta=\sum_{n=0}^{\infty}a_n\zeta^n$$

where a_n are real coefficients according to (11). We have on $|\zeta|=1$

$$\left.\begin{aligned}\tau&=\sum_{n=0}^{\infty}a_n\cos n\sigma\\ -\theta&=\sum_{n=1}^{\infty}a_n\sin n\sigma\end{aligned}\right\} \qquad (12)$$

In order to eliminate a_n from (12), we introduce a plausible assumption that if we know the values of $d\tau/d\sigma$ at sufficiently many points $\sigma=\sigma_j$

$$(0=\sigma_0<\sigma_1<\cdots\cdots<\sigma_N=\pi)$$

we can use the following approximation

$$\frac{d^2\tau}{d\sigma^2}=\frac{\eta_j-\eta_{j-1}}{\sigma_i-\sigma_{j-1}} \qquad (13)$$

in the interval

$$\sigma_{j-1}<\sigma<\sigma_j$$

where η_j denote the values of $d\tau/d\sigma$ at $\sigma=\sigma_j$.

Applying Fourier's theorem to

$$\frac{d^2\tau}{d\sigma^2}=-\sum_{n=1}^{\infty}n^2a_n\cos n\sigma$$

and substituting (13) into the left hand side, we have

$$\sum_{j=1}^{N}\frac{\eta_j-\eta_{j-1}}{\sigma_j-\sigma_{j-1}}\int_{\sigma_{j-1}}^{\sigma_j}\cos n\sigma=-\frac{\pi}{2}n^2a_n$$

and

$$\begin{aligned}-\theta_k&=\sum_{n=1}^{\infty}a_n\sin n\sigma_k\\ &=-\frac{2}{\pi}\sum_{j=1}^{N}\frac{\eta_i-\eta_{i-1}}{\sigma_j-\sigma_{j-1}}\sum_{n=1}^{\infty}\sin n\sigma_k\\ &\qquad(\sin n\sigma_j-\sin n\sigma_{j-1})/n^3\\ &=\sum_{j=1}^{N}\frac{\eta_j-\eta_{j-1}}{\sigma_j-\sigma_{j-1}}\{F(\sigma_k+\sigma_j)-F(\sigma_k-\sigma_j)\\ &\qquad-F(\sigma_k+\sigma_{j-1})+F(\sigma_k-\sigma_{j-1})\}\end{aligned} \qquad (14)$$

where

$$F(\rho)=\frac{1}{\pi}\sum_{n=1}^{\infty}\frac{\cos n\rho}{n^3} \qquad (15)$$

It is straightforward to reduce (14) to the simpler form

$$\theta_k=\sum_{j=1}^{N-1}\eta_jR_{jk} \qquad (16)$$

since $\eta_0=\eta_N=0$. As we have to carry out a few subtractions before each R_{jk} is obtained, it is better to calculate $F(\rho)$ with 'double precision'.

The infinite Fourier series (15) is summed by twice integrating

$$-\sum_{n=1}^{\infty}\frac{\cos n\rho}{n}=\log\left(2\sin\frac{\rho}{2}\right) \qquad (17)$$

With the help of

$$\log\sin\rho=\log\rho-\sum_{m=1}^{\infty}\frac{2^{2m-1}B_m\rho^{2m}}{(2m)!\,m} \qquad (18)$$

Table 1. Distributions of interval length used in numerical calculations of (1) deep water waves, (2) waves in intermediate depth, and (3) solitary waves. The unit of interval length is $\pi/7280$, $\pi/2400$, and $\pi/6890$, respectively.

(1)		(2)		(3)	
Interval length	j	Interval length	j	Interval length	j
1	1-20	1	1-15	1	1-17
3	21-40	3	16-30	3	18-34
9	41-60	9	31-45	9	35-51
27	61-80	27	46-60	27	52-68
81	81-100	81	61-75	81	69-85
243	101-120	27	76-90	243	86-102
		9	91-105	81	103-108
		3	106-120	27	109-114
				9	115-120

we obtain an approximate expression

$$\pi\cdot F(\rho)=\frac{\rho^2}{2}\left(\log\rho-\frac{3}{2}\right)-\sum_{m=1}^{10}\frac{B_m\,\rho^{2m+2}}{(2m+2)!\,2m} \tag{19}$$

where B_m are the Bernouilli's numbers. The formulas (17) and (18) are quoted from MORIGUCHI *et al.* (1957).

The accuracy of (16) can be estimated by a test function

$$\tau-i\theta=\log(1+\gamma-e^{i\sigma}) \tag{20}$$

which gives

$$\frac{d\tau}{d\sigma}=Re\left(\frac{-ie^{i\sigma}}{1+\gamma-e^{i\sigma}}\right) \tag{21}$$

We compare θ_k computed by (16) and (21) with the exact θ_k given by (20). We give such a γ that at least a few, say six, points are contained between $\sigma=0$ and the value of σ for which $d\tau/d\sigma$ is a maximum. When we use 120 points whose distribution is shown in Table 1, the relative error is about $-0.5\,\%$ at the first point, changes sign near the peak of $d\tau/d\sigma$, and becomes $0\sim0.1\,\%$ for $j>10$.

4. A method of iteration

The numerical solutions of (8) are labeled with a parameter b which is indirectly related to the wave amplitude. At each cycle of our iterative procedure the eigenvalue gL_0/U^2 is determined from the condition that b should have a specified value. We have empirically found that the definition

$$b=\sum_{j=1}^{N}(\xi_j-\xi_{j-1})^2/(\sigma_j-\sigma_{j-1}) \tag{22}$$

with

$$\hat{\xi}_j=\eta_j\sqrt{1+a^2-2a\cos\sigma_j}\sim\left.\frac{\partial\tau}{\partial\phi}\right|_{\phi=\phi_j}$$

gives an efficient iterative procedure whose convergence rate turns out to be insensitive to the amplitude of the solutions.

It is emphasized that the magnitude of b, which may be called a mean square derivative, depends a little on the resolving power of discrete points, even if we are dealing with an identical particular solution of (8). So b is regarded as an auxiliary parameter and we do not document its values here. In retrospect we think an alternative expression

$$b=\sum_{j=1}^{N}(\xi_j-\xi_{j-1})^2/(\phi_j-\phi_{j-1})$$

should have been preferred to (22), for ϕ has a clearer geometrical meaning than σ.

The details of our method are as follows:

4.1) Assign the numerical values of a and b, and give a first approximation to η_j.

4.2) Multiply η_j with such a constant that (22) is satisfied.

4.3) Calculate θ_j by (16) and τ_j by

$$\tau_{j-1}=\tau_j-(\eta_j+\eta_{j-1})(\sigma_j-\sigma_{j-1})/2$$

with $\tau_N=0$. (In the present work numerical integrations are always carried out by the trapezoidal rule.)

4.4) Using (8), calculate a new η_j by

$$\eta_j=\frac{gL_0}{U^2}\frac{\chi_j}{\sqrt{1+a^2-2a\cos\sigma}}$$

where

$$\chi_j=e^{-3\tau_j}\sin\theta_j$$

and

$$\frac{gL_0}{U^2}=\sqrt{b/\sum_{j=1}^{N}(\chi_j-\chi_{j-1})^2/(\sigma_j-\sigma_{j-1})} \qquad (23)$$

4.5) Subtract, for each j, the old η_j used in 4.3) from the new η_j obtained in 4.4). The maximum magnitude of the difference is called 'the maximum difference'. And if it is not permitted to stop the calculation according to a certain criterion, take the average of the old and new η_j, and return to the step 4.2).

The maximum difference usually becomes about 0.6 times its former value after one cycle of iteration, but sooner or later it begins to oscillate with a non-increasing amplitude. The peak value of this oscillation is called 'the final maximum difference ε'. And at this final stage the relative fluctuation of the eigenvalue gL_0/U^2 is less than 1×10^{-4}. It is regrettable that we do not yet know whether the final maximum difference ε can be made smaller by increasing the significant digits of the numerical calculation.

5. Definition of various physical quantities

The following symbols are used in tabulating the results:

L ; wave length
H ; wave height, or vertical distance from a wave crest to a wave trough
C ; wave velocity
D ; vertical distance from the bottom to a wave trough
D_M ; mean depth
L_I ; interpolated horizontal distance from the wave crest to the inflection point of a wave profile
H_I ; interpolated vertical distance from the wave crest to the inflection point of a wave profile
θ_M ; interpolated maximum value of θ, the surface slope angle
j_1 ; location of the point where θ_j is maximum
B ; maximum value of $d\tau/d\sigma$
j_2 ; location of the point where $d\tau/d\sigma$ is maximum
V_C ; orbital velocity (due to wave) at the crest
Q ; mass transport of wave
δ_S ; drift of a surface particle per cycle of its orbit
A_C ; normal acceleration of a particle at the wave crest
ε ; final maximum difference

As usually done, the relevant physical quantities are non-dimensionalized by suitable combinations of L, D and g. For this purpose we eliminate U and L_0 by (23) and

$$\frac{L}{2L_0}=\int_0^{\pi}\frac{e^{-\tau}\cos\theta\,d\sigma}{\sqrt{1+a^2-2a\cos\sigma}} \qquad (24)$$

respectively.

The normal acceleration of a fluid particle on the free surface is (square of velocity)$\times$ (curvature of surface)

$$=\frac{U^2}{L_0}e^{3\tau}\sqrt{1+a^2-2a\cos\sigma}\frac{d\theta}{d\sigma} \qquad (25)$$

where we approximate $d\theta/d\sigma$ by $(\theta_j-\theta_{j-1})/(\sigma_j-\sigma_{j-1})$.

The wave velocity C is defined as the relative velocity of the wave crest to an observer to whom the time average fluid velocity vanishes on the bottom, that is,

$$C=\frac{2}{L}\int_{\phi_T}^{\phi_C}Ue^{\tau}\frac{e^{-\tau}}{U}d\phi=2(\phi_C-\phi_T)/L \qquad (26)$$

In deriving this expression we have utilized the relation of a time average (for a uniformly moving observer) to a space average.

Concerning the mean motion of fluid particles, we use well known expressions for the drift

$$\delta(\phi)=C\cdot T(\phi)-L \qquad (27)$$

and the mass transport velocity

$$u_*=C-L/T(\phi)=C\cdot\delta/(L+\delta)$$

where

$$T(\phi)=2\int_{\phi_T}^{\phi_C}\left(\frac{x_\phi^2+y_\phi^2}{u^2+v^2}\right)^{1/2}d\phi=\frac{2}{C_0^2}\int_{\phi_T}^{\phi_C}e^{-2\tau}d\phi$$

And the mass transport is given by

$$\begin{aligned}Q&=\frac{2}{L}\int_{\phi_B}^{\phi_S}\left(C-\frac{L}{T(\phi)}\right)\frac{\partial(x,y)}{\partial(\phi,\psi)}\,d\psi\,d\phi\\&=C\cdot D_M-\phi_S+\phi_B\\&=CL\left\{\frac{D_M}{L}-\frac{\phi_S-\phi_B}{2(\phi_C-\phi_T)}\right\}\end{aligned}\qquad(28)$$

which was derived by YAMADA (1958).

6. Calculation of depth

The evaluation of mass transport by (28) requires an accurate value of D_M/L for each wave. Therefore it is necessary to know the vertical distance from the bottom to some point on the free surface. After $d(\phi+i\psi)$ is eliminated from (2) and (5), the resulting expression is numerically integrated from $\zeta=-0.2$ to the 83rd point (located approximately at $\sigma=5\pi/6$). The path of integration is a straight line drawn between the end points. Actually (10) is also evaluated on this path.

The value of $\tau-i\theta$ at twenty points uniformly distributed on the path are calculated by

$$\begin{aligned}\tau(\zeta)-i\theta(\zeta)=&-\frac{i}{2\pi}\sum_{j=1}^{N-1}\eta_j(\sigma_{j+1}-\sigma_{j-1})\\&\times\log\frac{(\zeta e^{-i\sigma_j}-1)(e^{i\sigma_j}+1)}{(e^{-i\sigma_j}+1)(\zeta e^{i\sigma_j}-1)}\end{aligned}\qquad(29)$$

The essential properties of $\tau-i\theta$ utilized in constructing this expression are that it is an analytic function in $|\zeta|<1$, that it satisfies (11), that its real part has a jump at $\zeta=e^{i\sigma_j}$, the magnitude of which is $\eta_j(\sigma_{j+1}-\sigma_{j-1})/2$, and that $\tau=0$ at $\zeta=-1$. Though the third of these conditions is a worse approximation than (13), it has been adopted for simplicity.

7. Presentation of results

Table 1 shows the distributions of interval length used in the calculation. Table 2 shows the characteristics of very steep deep water waves. Table 3 shows those of very steep solitary waves. And Table 4 to Table 7 show the characteristics of fairly steep waves.

Figure 2 shows the location of the inflection point of wave profiles versus the maximum surface slope angle. Figure 3 shows the orbital velocity due to wave motion at the wave crest. Figure 4 shows the distribution of surface slope angle near the inflection points of solitary waves. In Figure 5, the calculated phase velocity of deep water waves is compared with the Stokes' second and fourth approximation.

The Stokes' fourth approximation is parametrically represented by

$$\frac{H}{L}=\frac{\alpha}{\pi}\left(1+\frac{3}{8}\alpha^2\right)$$

and

$$\frac{2\pi C^2}{gL}=1+\alpha^2+\frac{5}{4}\alpha^4$$

(See KINSMAN, 1965). It is not necessary to

Table 2. Characteristics of very steep waves in deep water. ($a=0.0$)

θ_M	0.5091	0.5116	0.5133	0.5146	0.5157	0.5165	0.5173	0.5179
j_1	43	41	40	38	38	34	33	32
B	41.8	50.6	58.8	66.5	73.6	80.6	87.1	93.7
j_2	11	9	8	7	7	6	5	5
H/L	0.1390	0.1392	0.1394	0.1395	0.1396	0.1397	0.1398	0.1398
$C\sqrt{2\pi/gL}$	1.0933	1.0932	1.0932	1.0931	1.0931	1.0931	1.0930	1.0930
L_1/H	0.1757	0.1602	0.1490	0.1393	0.1318	0.1256	0.1202	0.1156
H_1/H	0.0781	0.0721	0.0677	0.0636	0.0605	0.0578	0.0556	0.0536
Vc/C	0.8421	0.8514	0.8586	0.8642	0.8688	0.8727	0.8759	0.8788
$\delta s/H$	2.209	2.236	2.255	2.271	2.284	2.294	2.304	2.312
Ac/g	0.382	0.382	0.382	0.382	0.381	0.380	0.380	0.379
$\varepsilon\times10^5$	5	5	6	8	8	9	11	11

Table 3. Characteristics of very steep solitary waves. ($a=-1.0$)

θ_M	0.5156	0.5174	0.5186	0.5196	0.5203	0.5209	0.5214	0.5218
i_1	39	37	36	35	34	34	32	31
B	41.8	50.7	58.7	66.4	73.8	80.4	87.4	93.7
i_2	11	9	8	7	6	6	5	5
H/D	0.8187	0.8195	0.8201	0.8205	0.8209	0.8211	0.8214	0.8216
$C/\sqrt{gD}$	1.2859	1.2858	1.2858	1.2857	1.2857	1.2857	1.2857	1.2856
L_1/H	0.1062	0.0959	0.0888	0.0835	0.0793	0.0757	0.0722	0.0694
H_1/H	0.0486	0.0443	0.0413	0.0391	0.0373	0.0357	0.0341	0.0329
Vc/C	0.9029	0.9089	0.9133	0.9168	0.9195	0.9219	0.9239	0.9257
$\delta s/H$	4.655	4.678	4.695	4.708	4.719	4.729	4.737	4.744
Ac/g	0.384	0.383	0.383	0.382	0.382	0.381	0.380	0.379
$\varepsilon\times10^5$	8	8	5	9	14	10	15	15

Table 4. Characteristics of steep waves in deep water. ($a=0.0$)

θ_M	0.5025	0.4933	0.4812	0.4658	0.4459	0.4208	0.3891
H/L	0.1383	0.1373	0.1357	0.1334	0.1299	0.1248	0.1174
$C\sqrt{2\pi/gL}$	1.0932	1.0928	1.0918	1.0896	1.0857	1.0894	1.0704
$\delta s/H$	2.143	2.062	1.964	1.885	1.727	1.583	1.416

Table 5. Characteristics of steep, solitary waves. ($a=-1.0$)

θ_M	0.5103	0.5034	0.4879	0.4619	0.4265	0.3705	0.3004
H/D	0.8164	0.8133	0.8058	0.7909	0.7650	0.7113	0.6254
$C/\sqrt{gD}$	1.2863	1.2868	1.2880	1.2890	1.2874	1.2774	1.2534
$\delta s/H$	4.595	4.528	4.409	4.266	4.134	4.010	3.955

Table 6. Characteristics of steep waves in medium depth. ($a=-0.9$) $(\psi_S-\psi_B)/2(\phi_C-\phi_T)=0.1813$

θ_M	0.5106	0.5038	0.4883	0.4627	0.4511	0.4274	0.3978	0.3480
H/D	0.6678	0.6651	0.6584	0.6445	0.6371	0.6197	0.5941	0.5427
H/L	0.1097	0.1093	0.1081	0.1058	0.1045	0.1016	0.0974	0.0891
$C/\sqrt{gD}$	0.9806	0.9808	0.9809	0.9795	0.9782	0.9748	0.9689	0.9563
Q/CL	0.0144	0.0145	0.0146	0.0146	0.0146	0.0146	0.0143	0.0134
$\delta s/H$	2.307	2.245	2.114	1.943	1.867	1.734	1.583	1.358

Table 7. Characteristics of steep waves in medium depth. ($a=-0.98$) $(\psi_S-\psi_B)/2(\phi_C-\phi_T)=0.1312$

θ_M	0.5104	0.5036	0.4880	0.4622	0.4506	0.4268	0.3971	0.3473
H/D	0.7417	0.7388	0.7317	0.7173	0.7098	0.6923	0.6665	0.6150
H/L	0.0893	0 0889	0.0880	0.0862	0.0853	0.0831	0.0800	0.0738
$C/\sqrt{gD}$	1.0598	1.0600	1.0602	1.0593	1.0583	1.0553	1.0498	1.0377
Q/CL	0.0110	0.0110	0.0111	0.0111	0.0112	0.0113	0.0110	0.0105
$\delta s/H$	2.398	2.330	2.203	2.027	1.959	1.826	1.690	1.444

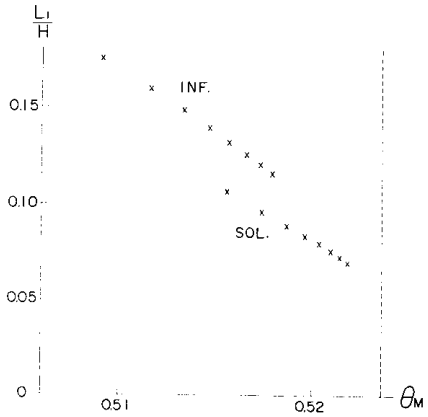

Fig. 2. Location of inflection points of wave profiles. L_1, H and θ_M are the horizontal distance from a wave crest to the nearest inflection point of the wave profile, wave height, and the maximum value of the surface slope angle, respectively. A dotted vertical line corresponds to $\theta_M=\pi/6$. The symbols *SOL.* and *INF.* denote solitary waves and deep water waves, respectively.

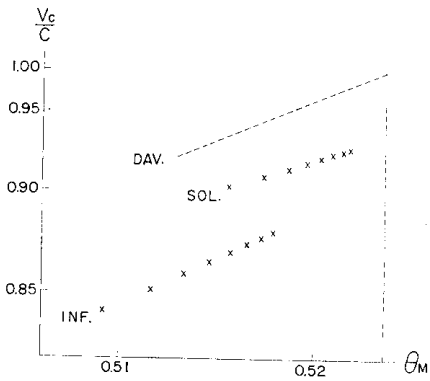

Fig. 3. Particle velocity at the crest of waves. Vc, C and θ_M are the particle velocity due to wave motion at wave crest, wave velocity, and the maximum value of the surface slope angle, respectively. A dotted vertical line corresponds to $\theta_M=\pi/6$. The symbols *DAV.*, *SOL.* and *INF.* denote the relation (32) derived from Davies' exact solution, solitary waves, and deep water waves, respectively.

eliminate α from these expressions, since the comparison with numerical results is made graphically.

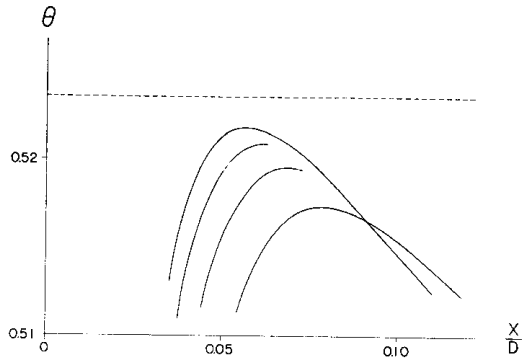

Fig. 4. Distributions of the surface slope angle θ of solitary waves, whose heights are 0.8216D, 0.8211 D, 0.8205 D, and 0.8195 D. A dotted horizontal line corresponds to $\theta=\pi/6$.

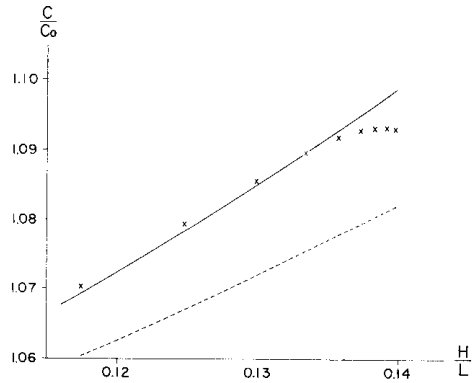

Fig. 5. Comparison of the wave velocity of deep water waves. C/C_0 denotes wave velocity divided by $\sqrt{gL/2\pi}$ and H/L denotes wave steepness. Crossed points are calculated values, the solid curve is Stokes' fourth approximation, and the dotted curve is his second approximation.

8. Application of our method to Davies' equation

DAVIES (1951) pointed out that an analytic function

$$\tau-i\theta=\frac{1}{3}\log(1-Ae^{-iw}) \qquad (30)$$

of a complex variable w is the solution of a differential equation

$$\frac{d(\tau-i\theta)}{dw}=\frac{i}{3}\{e^{-(\tau-i\theta)}-1\}$$

Table 8. Characteristics of numerical solutions of Davies' equation.

θ_M	0.490	0.494	0.498	0.502	0.506
A	0.99493	0.99606	0.99705	0.99790	0.99860
$1/3(1+A)$	0.16709	0.16700	0.16691	0.16684	0.16678
$(1+A)^{1/3}$	1.25886	1.25909	1.25930	1.25948	1.25963
eigenvalue	0.16696	0.16686	0.16678	0.16671	0.16665
$L/2\pi L_0$	1.25902	1.25926	1.25947	1.25964	1.25979
j_1	57	54	51	48	44
B	32.8	41.6	56.5	79.6	119.9
j_2	12	11	7	5	3
$10^5\times\varepsilon$	6	6	8	8	14

whose real part gives

$$\frac{d\tau}{d\sigma}=\frac{1}{3}e^{-3\tau}\sin 3\theta \qquad (31)$$

where

$$\sigma=-Re(w)$$

Equation (31), which we call Davies' equation, is obviously very much similar to (8) in the case $a=0$. Starting from this fact, DAVIES carried out a unique perturbation calculation on the waves near the limiting condition. But we do not think his result to be conclusive, and only make use of the similarity between (31) and (8), in order to estimate the accuracy of our numerical solutions of Equation (8).

We consider the behavior of τ and θ an the line $Im(w)=0$. Then we have

$$\left.\begin{array}{l} A=\sin 3\theta_M \\ \text{or} \\ 1-A=2\sin^2\{(\pi/2-3\theta_M)/2\} \end{array}\right\} \qquad (32)$$

where θ_M is the maximum of θ. (This relation is immediately found, if one draws a vector $1-Ae^{i\sigma}$ in a complex plane.) In this case the quantity $1-V_C/C=Ue^{\tau}/C$ can be exactly calculated. From (30) we have $e^{3\tau}=1-A$ at $\sigma=0$, and from (9), (24), and (26) we have $U/C=1$. The resulting expression is

$$(1-V_C/C)^{3/2}=\sqrt{2}\sin\{(\pi/2-3\theta_M)/2\} \qquad (33)$$

which is shown in Figure 3 with a symbol DAV.

In our calculation we have assumed that $\tau=0$ at $\sigma=\pi$. Therefore we change (30) and (31) into

$$\tau-i\theta=\frac{1}{3}\log\{(1-Ae^{-i\sigma})/(1+A)\} \qquad (30)'$$

and

$$\frac{d\tau}{d\sigma}=\frac{1}{3(1+A)}e^{-3\tau}\sin 3\theta \qquad (31)'$$

respectively. We give θ_M and the exact solution of (31)′ is determined by (30)′ and (32), while the numerical solution of (31)′ is calculated by the procedure described in Section 4 with the condition that its mean square derivative defined in (22) is identical with that of the exact solution. (It is necessary to put $a=0$ and to use $\chi_j=e^{-3\tau_j}\sin 3\theta_j$ instead of $\chi_j=e^{-3\tau_j}\sin\theta_j$.)

A few features of the solutions are shown in Table 8, and the relative errors of θ at the

Table 9. Relative errors of θ at selected points. The θ calculated by our method is compared with the exact value given by (30′).

	$\theta_M=0.502$	$\theta_M=0.498$
j		
1	−0.0056	−0.0031
3	−0.0024	−0.0020
5	−0.0001	−0.0007
7	0.0012	0.0002
9	0.0015	0.0006
11	0.0016	0.0008
21	0.0014	0.0010
31	0.0005	0.0004
41	0.0004	0.0004
51	0.0001	0.0001

selected points are listed in Table 9. In all the case shown in Table 8 we have found that the numerical solutions of (31)′ converge to the exact solution (30)′ with small errors as shown typically in Table 9, that the eigenvalues calculated by (23) are about 0.08 % smaller than the exact value $1/3(1+A)$, and that the ratio $L/2\pi L_0$ calculated by (24) is about 0.013 % greater than the exact value $(1+A)^{1/3}$.

9. Discussion and summary

The primary source of errors in our results is that calculations are carried out with a finite number of points distributed on $|\zeta|=1$. To obtain as much resolving power as possible, non-uniform distributions of points are provided as shown in Table 1. With the same number of points or the same amount of computation, the density of points near the wave crest ($\zeta=1$) can be made nearly one hundred times larger than the density that is attained by means of a uniform distribution of points. We have described in Section 3 a convenient way of deriving the explicit relation (16) between $d\tau/d\sigma$ and θ for a given distribution. By applying (16) to the test function (20) we can readily estimate the dependence of errors on the behavior of analytic functions and the distribution of points.

The knowledge of the exact solution of Davies' Equation (31)′ is very important to demonstrating the reliability of our method as a whole. From Table 8 and Table 9 we can draw two conclusions. First, the existence of a few, say five or more, points between $\sigma=0$ and the peak of $d\tau/d\sigma$ is necessary for the results of our iterative calculations to be very close to the exact solution. Second, the magnitude of error in gL_0/U^2 and L/L_0 is very small (less than 0.1 %).

The phase velocity C in Table 2 is calculated by

$$C\sqrt{\frac{2\pi}{gL}}=\left(\frac{U^2}{gL_0}\right)^{1/2}\left(\frac{2\pi L_0}{L}\right)^{3/2}$$

which is derived from (9) and (26). Relying on the similarity of (8) to (31)′, we assume that the systematic errors in gL_0/U^2 and L/L_0 are -0.08 % and 0.013 %, respectively also in the case of numerical solutions of Equation (8). Then the systematic error in C is about 0.02 %. Therefore, the departure of the calculated phase velocity from the Stokes' fourth approximation, as shown in Figure 5, is concluded to be a genuine feature.

Suppose that there are two distributions of $d\tau/d\sigma$ calculated by our method, of which one is a numerical solution of Equation (31)′ and the other is that of Equation (8). Suppose that the peak of the former is nearer to $\sigma=0$ than the peak of the latter, so that insufficient resolving power or a possible defect in our method produces larger errors in the former than in the latter. And suppose that the former is very close to an exact solution of (31)′. Then there is no reason to suspect that the latter is not an accurate solution of (8). We emphasize that the similarity of Equation (8) to Equation (31)′ is remarkable even when $a\neq 0$, and that based on the arguments given above the relative errors of our solutions of (8) are approximately the same as shown in Table 8 and Table 9. But we should also note that our results for solitary waves are a little sensitive to the density of points near the tail of waves.

In Figure 3 we use such a scaling of $1-V_C/C$ that Equation (33) is represented by a straight line. The plotted points in Figure 3 showing the relation between θ_M and V_C/C of solitary waves and deep water waves seem also to lie on straight lines. By extrapolation we anticipate that we shall be able to calculate the solutions of (8) with $\theta_M>\pi/6$ and $V_C<C$. (The condition $V_C<C$, which means that the wave is physically possible, corresponds to the finiteness of τ in the present problem.) And the maximum points of θ in Figure 4 seem also to lie on a straight line which crosses the dotted line ($\theta=\pi/6$). Therefore, at present we do not accept the proposition that steady state waves with $\theta>\pi/6$ do not exist at all, which was put forward by KRASOVSKII (1961) without proof. But it should be noted that as the breaking condition is approached, θ_M may begin to decrease and the condition $\theta_M=\pi/6$ at $V_C=C$ may be realized.

The replacement of $d\theta/d\sigma$ with $\Delta\theta/\Delta\sigma$ in the expression (25) brings forth a systematic error.

Consider for example a test function (30), which can be made close to any of our numerical solutions. At $\sigma=0$ we have

$$d\theta/d\sigma=A/3(1-A)$$

while our numerical approximation gives

$$(\theta_1-0)/(\sigma_1-0)\doteqdot A/3(1-A\cos\sigma_1)$$

The relative error is given by

$$(\theta_1/\sigma_1)/(d\theta_1/d\sigma_1)-1=A(\cos\sigma_1-1)/(1-A\cos\sigma_1)$$
$$\doteqdot -\sigma_1^2/\{(\pi/2-3\theta_M)^2+\sigma_1^2\}$$

where we have used (32) and have assumed that $\sigma_1\ll 1$ and $\pi/2-3\theta_M\ll 1$. If we put $\sigma_1=\pi/7280$ and $\theta_M=0.52$, the error is $-0.2\,\%$. Therefore, the error in the normal particle acceleration at the wave crest is concluded to be less than $1\,\%$.

LONGUETT-HIGGINS (1963) estimated the normal acceleration at the crest of the limiting wave. Instead of $C^2=1.5\,gL/2\pi$ (his Equation 4.7) we use $C=1.093\sqrt{gL/2\pi}$ given in Table 2, and use his Equation 4.13 to obtain $A_C=-0.40\,g$, while Table 2 and Table 3 give $A_C=-0.38\,g$. This fair agreement shows that our numerical solutions can be approximated by (30), which correspods to his Equation 4.2, in so far as the accceleration is concerned.

YAMADA (1958) has calculated the mass transport of only one wave with $\theta_M=\pi/6$ and $D_M/L=0.260$. The magnitude of the mass transport given in Table 6 and Table 7 is a little too large compared with the value of $Q/CL=0.0087$ obtained by YAMADA. Our results for mass transport are considered to be of a preliminary nature, since a careful examination of the error due to (29) has not yet been carried out.

Acknowledgments

The present study was carried out under the supervision and with the encouragement of Professor Kozo YOSHIDA, to whom we express our sincere gratitude. We thank Associate Professor Yutaka NAGATA for giving valuable comments and for correcting illogical statements in the manuscript. And we thank Dr. Harold SOLOMON who kindly pointed out our elementary mistakes in English. (But he is not responsible for those parts which were modified after the time of his reading.)

Numerical calculations were carried out at the Computer Center of the University of Tokyo.

References

BYATT-SMITH, J. G. B. (1970): An exact integral equation for steady surface waves. Proc. Roy. Soc. London A, **315**, 405-418.

CHAPPELEAR, J.E. (1959): On the theory of highest waves. Beach Erosion Board, Tec. Mem., **116**, 1-28.

CHAPPELEAR, J.E. (1961): Direct numerical calculation of wave properties. J. Geophys. Res., **66**, 501-508.

DAVIES, T.V. (1951): The theory of symmetrical gravity waves of finite amplitude. I. Proc. Roy. Soc. London A, **208**, 475-486.

FENTON, J. (1972): A ninth-order solution for the solitary wave. J. Fluid Mech., **53**, 257-271.

KINSMAN, B. (1965): Wind waves. Prentice Hall, Englewood Cliffs, N.J.

KRASOVSKII, Yu P. (1961): On the theory of permanent waves of finite amplitude. Zh. Vychisl. Mat. i Mat. Fiz., **1**, 836-855.

LENAU, C.W, (1966): The solitary wave of maximum amplitude. J. Fluid Mech., **26**, 309-320.

LONGUETT-HIGGINS, M.S. (1963): The generation of capillary waves by steep gravity waves. J. Fluid Mech., **16**, 138-156.

MCCOWAN, J. (1894): On the highest wave of permanent type. Phil. Mag., Series 5, **38**, 351-358.

MICHELL, J.H. (1893): The highest waves in water. Phil. Mag., Series 5, **36**, 430-437.

MORIGUCHI, S., K. UDAGAWA, and S. HITOTSUMATSU (1957): A collection of mathematical formulas. II. (in Japanese) Iwanami and Co., Hitotsubashi Tokyo.

VON SCHWIND, J.J., and R.O. REID (1972): Characteristics of gravity waves of permanent form. J. Geophys. Res., **77**, 420-433.

YAMADA, H. (1957): Highest waves of permanent type on the surface of deep water. Rep. Res. Inst. Appl. Mech. Koushu Univ., **5**, 37-52.

YAMADA, H. (1957): On the highest solitary wave. Rep. Res. Inst. Appl. Mech. Kyushu Univ., **5**,

53-67.
YAMADA, H. (1958): Permanent gravity waves on water of uniform depth. Rep. Res. Inst. Appl. Mech. Kyushu Univ., **6**, 127-139.

極限波高に近い，進行する，うずなしの，水面重力波について

佐々木　建，村上　敬

要旨：一定水深の水の表面を進行する渦なし重力波の数値解をくり返し法で求めた．その結果は，水面傾斜角が30°をこえるような波の存在を示唆する．計算された深水波の波速は，波形勾配 0.14 の附近で，ストークスの第4近似が与える波速よりもかなり小さくなる．

われわれの計算法の信頼性を検証するために，DAVIES (1951) の提案した問題にそれを適用した．彼の問題は仮想的なものであるが，本論文の主題とよく似ている．そしてその厳密解が知られている．この場合，計算結果は厳密解とよく一致した．